Secretory Carrier Membrane Protein SCAMP2 and Phosphatidylinositol 4,5-Bisphosphate Interactions in the Regulation of Dense Core Vesicle Exocytosis†

Haini Liao,‡,§ Jeff Ellena,|| Lixia Liu,‡ Gabor Szabo,⊥ David Cafiso,|| and David Castle*,‡,§

Departments of Cell Biology, Chemistry, Molecular Physiology, and Biological Physics and the Cell and Developmental Biology Program, University of Virginia, Charlottesville, Virginia 22908

Received June 6, 2007; Revised Manuscript Received July 19, 2007

ABSTRACT: Secretory carrier membrane protein 2 (SCAMP2) functions in late steps of membrane fusion in calcium-dependent granule exocytosis. A basic/hydrophobic peptide segment within SCAMP2 (SCAMP2 E: CWYRPIYKAFR) has been implicated in this function and shown to bind and sequester phosphatidylinositol 4,5-bisphosphate [PI(4,5)P_2 or PIP_2] within membranes through an electrostatic mechanism. We now show that alanine substitution of tryptophan W2 within SCAMP2 E substantially weakens peptide binding to negatively charged liposomes; other substitutions for arginine R4 and lysine K8 have only limited effects on binding. Electron paramagnetic resonance analysis of liposomes containing spin-labeled PIP_2 shows that R4 but not K8 is critical for SCAMP E binding to PIP_2. The interfacial locations of SCAMP E and its structural variants within lipid bicelles measured by oxygen enhancement of nuclear relaxation are all similar. Corresponding point mutations within full-length SCAMP2 (SC2-R204A, SC2-K208A, and SC2-W202A) have been analyzed for biological effects on dense core vesicle exocytosis in neuroendocrine PC12 cells. With the same level of overexpression, SC2-R204A but not SC2-K208A inhibited secretion of cotransfected human growth hormone and of noradrenalin. Inhibition by SC2-R204A was the same as or greater than previously observed for SC2-W202A. Analysis of noradrenalin secretion by amperometry showed that inhibitory mutants of SCAMP2 decrease the probability of fusion pore opening and the stability of initially opened but not yet expanded fusion pores. The strong correlation between SCAMP2 E interactions with PIP_2 and inhibition of exocytosis, particularly by SC2-R204A, led us to propose that SCAMP2 interaction with PIP_2 within the membrane interface regulates fusion pore formation during exocytosis.

Phosphatidylinositol phosphates (PIPs[1]) are reversibly phosphorylated derivatives of phosphatidylinositol that are distributed among cytoplasmic leaflets of cellular membranes. Despite their relatively low abundance, it has become clear that they play critical roles in organizing cellular activities that occur at membrane interfaces. At least seven different PIPs have been identified encompassing mono-, di-, and triphosphorylated derivatives of the myoinositol headgroup. The individual PIPs have distinct distributions among cellular organelles where they collaborate with other organelle-specific proteins (e.g., Rabs) to compartmentalize functions at specific locations (*1*). Phosphatidylinositol 4,5-bisphosphate [PI(4,5)P_2 or PIP_2], the most extensively investigated PIP, is concentrated in the plasma membrane where it constitutes ∼1% of total phospholipids. It functions in classical signal transduction and regulates an array of activities including the functions of several integral membrane proteins, dynamics of the cortical cytoskeleton and cell adhesion, and membrane interactions involved in exo- and endocytosis (*1*−*3*).

In regulated exocytosis in neuroendocrine cells, which is the focus of the present study, PIP_2 has been implicated as an essential regulatory component of the exocytotic machinery. The pleckstrin homology domain of phospholipase Cδ (PH-PLCδ), which specifically binds PIP_2, is an effective inhibitor of dense core vesicle (DCV) exocytosis in adrenal chromaffin cells (*4*). Further, depletion of plasma membrane PIP_2 by redistributing the PIP_2 biosynthetic enzyme phosphatidylinositol 4-phosphate 5-kinase (PIP5K-1γ) also inhibits DCV exocytosis (*5*). A variety of studies have pointed more specifically to a role of PIP_2 in ATP-dependent priming of DCVs in advance of Ca^{2+}-triggered fusion (*6*−*8*); other findings have implicated PIP_2 in organizing and expediting the Ca^{2+}-stimulated fusion step (*9*, *10*). There is also evidence from PIP5K-deficient chromaffin cells that PIP_2 may act still later to regulate the expansion of exocytotic fusion pores (*11*). Recent studies have highlighted local concentration of PIP_2 in microdomains (*12*) that serve in part as plasmalemmal docking sites for DCVs (*8*, *13*). However, there is presently little insight regarding how such microdomains are formed and stabilized in support of the ensuing fusion events.

† This work was supported by grants from the NIH (DE09655, DK077380, GM62305).

* To whom correspondence should be addressed. Tel: (434)-924-1786. Fax: (434)-982-3912. E-mail: jdc4r@virginia.edu.

‡ Department of Cell Biology.

§ Cell and Developmental Biology Program.

|| Department of Chemistry.

⊥ Departments of Molecular Physiology and Biological Physics.

[1] Abbreviations: PIP, phosphatidylinositol phosphate; PI(4,5)P_2 or PIP_2, phosphatidylinositol 4,5-bisphosphate; PIP5K-1γ, phosphatidylinositol 4-phosphate 5-kinase; PH-PLCδ, phospholipase Cδ ; DCV, dense core vesicle; SCAMP, secretory carrier membrane protein; hGH, human growth hormone; SAF, stand-alone-foot; PSF, prespike foot.

10.1021/bi701121j CCC: $37.00
Published on Web 08/22/2007

We have been interested in the possibility that secretory carrier membrane proteins (SCAMPs) might provide one of the functional connections between PIP_2 and DCV exocytosis. SCAMPs are integral membrane proteins with four transmembrane spans that reside mainly in membranes functioning in cell surface recycling (*14*, *15*). While four distinct SCAMPs are expressed ubiquitously in mammalian cells with a fifth isoform expressed in neural and neuroendocrine cells (*15*, *16*), two of the SCAMPs, SCAMPs 1 and 2, have been implicated as participants in exocytosis (*17*−*20*). In particular, our studies in neuroendocrine PC12 cells have shown that plasma membrane-associated SCAMP2 is concentrated in substantial part at sites enriched in the t-SNARE syntaxin1 and where DCVs are docked and that it functions in DCV exocytosis (*19*). More recently, we provided evidence that SCAMP2 appears to support exocytosis at two distinct levels. First, it serves as a scaffold for Arf6-GTP, phospholipase D1 (PLD1), and PIP5K ((*20*); our unpublished data). This machinery collaborates to produce phosphatidic acid (PA) and $PI(4,5)P_2$ required for exocytosis and associated with priming (*5*, *21*, *22*). Moreover, an Arf6 mutant that is specifically defective in activating PLD1 inhibits DCV exocytosis in a manner that is extremely similar to a subset of the inhibitory effects caused by an exocytosis-inhibiting SCAMP2 mutant (*20*), suggesting that the two mutants affect the same process. Second, SCAMP2 appears to have a role in facilitating dilation of fusion pores following their initial opening (*20*). In this case, the SCAMP2 mutant (but not the Arf6 mutant) destabilized fusion pores favoring their closure rather than dilation. We have been wondering whether the latter effect might relate to a direct association of SCAMP2 with PIP_2.

The SCAMP2 mutant used to analyze DCV exocytosis contained a single amino acid change W202A in the E peptide segment. In the full-length protein, E peptide constitutes most of the link between the second and third transmembrane spans (*23*). Topologically, it faces the cytoplasm and its extensive conservation, both among SCAMP isoforms and evolutionarily, suggests that it is a critical component of SCAMP function. SCAMP2 E peptide—CWYRPIYKAFR—is enriched in basic and aromatic residues, a composition that is characteristic of a variety of peptide segments of proteins that bind to membranes and regulate the distribution of polyanionic phospholipids, particularly PIP_2, by an electrostatic association (*3*). Previous studies have shown that synthetic SCAMP2 E peptide binds to membranes and that arginine residues R4 and R11 localize near the surface where they laterally sequester PIP_2 and prevent its hydrolysis by PLCδ (*24*, *25*). In the present study, we have sought to extend these observations by examining how selected structural variants of E peptide bind to membranes and associate with PIP_2 and to evaluate to what extent these interactions correlate with effects of corresponding point mutations of SCAMP2 on DCV exocytosis. In particular, we have focused on residues tryptophan W2, arginine R4, and lysine K8 (W202, R204, and K208 in full-length SCAMP2). Alanine substitution of W2 reduces membrane binding whereas substitutions of W2 and R4, but not K8, substantially reduce interactions with PIP_2. These effects correlate very well with the inhibitory effects of the corresponding point mutations of SCAMP2 on DCV exocytosis.

MATERIALS AND METHODS

Reagents. All lipids were from Avanti Polar Lipids (Alabaster, AL). The human SCAMP-derived E peptides include SCAMP1-WT (CWYRPLYGAFR), SCAMP2-WT (CWYRPIYKAFR), SCAMP2-W2A (CAYRPIYKAFR), and SCAMP2-R4A (CWYAPIYKAFR). The peptides with N-terminal acetylation and C-terminal amidation were synthesized by the Biomolecular Research Facility (UVA). Purity and composition were confirmed by HPLC and mass spectrometry. Proxyl-$PI(4,5)P_2$ was from Echelon Biosciences (Salt Lake City, UT). 4,4′-Dithiopyridine and noradrenalin (NA) were from Sigma-Aldrich (St. Louis, MO). Plasmid pTRE2 was from BD Biosciences Clontech (Palo Alto, CA), and bicistronic MSCV-based pIRES-EGFP vector was from Derek Persons (St. Jude's Children's Research Hospital, Memphis, TN). Enzyme-linked immunosorbent assay (ELISA) kits for human growth hormone secretion were from Roche Molecular Biochemicals (Hertfordshire, U.K.). Carbon fiber electrodes (CPE-1) were from ALA Scientific (Westbury, NY). N-terminal Myc-tagged SCAMP2, wild type and mutants (rat sequence) were subcloned into pIRES-EGFP, *Nhe*I and *Xho*I sites (*19*, *20*).

Vesicle Preparations. Sucrose-loaded large unilamellar vesicles (LUVs) were used for peptide binding measurements made by centrifugation. The vesicles were formed from palmitoyloleoylphosphatidylcholine (PC), palmitoyloleoylphosphatidylserine (PS), and $PI(4,5)P_2$ (79.9:20:0.1). After removing chloroform by vacuum desiccation, the resulting lipid film was hydrated in 176 mM sucrose, 1 mM 3-morpholinopropanesulfonic acid (MOPS), and 100 mM KCl, pH 7.0. To prepare LUVs, the hydrated lipid was subjected to five cycles of freezing and thawing followed by 19−25 cycles through 100 nm polycarbonate filters using a LipoFast extruder (Avestin, Ottawa, Canada). The LUVs used for EPR were formed from PC. The desiccated lipid film was hydrated in sucrose-free 100 mM KCl, 1 mM MOPS, pH 7.0 to a final concentration of 20−25 mM PC and treated as for sucrose-loaded LUVs. The proxyl-$PI(4,5)P_2$ was incorporated into the outer leaflet of the vesicles by adding the preformed lipid vesicles to a dried aliquot of the spin label, which was ~0.25 mol % of the total lipid.

Centrifugation Binding Measurements. The centrifugation technique has been described previously (*24*, *25*). Sucrose-loaded LUVs were washed with 5 volumes of 100 mM KCl, 1 mM MOPS (pH 7.0) by centrifugation and resuspended in fresh buffer. Different concentrations of sucrose-loaded LUVs (0.05−20 mM lipid) were mixed with 10 μM SCAMP E peptides ([lipid] ≫ [peptide]) and were centrifuged at 100000*g* for 1 h to pellet the LUVs. Supernatants were withdrawn, and aliquots were mixed with 200 μM 4,4′-dithiodipyridine (4-PDS) to measure unsedimented peptide by its N-terminal cysteine spectrophotometrically (*26*). Controls included KCl−MOPS buffer (blank); supernatants from vesicles (10 mM) pelleted in the absence of peptide (which gave negligible OD_{324}), and the plot of OD_{324} as a function of peptide concentration was satisfactory. Binding was expressed as a reciprocal molar binding constant K as given by

$$F_{\text{bound}} = \frac{K[\text{L}]}{1 + K[\text{L}]} \quad (1)$$

F_{bound} is the fraction of peptide bound to vesicle membranes; [L] represents the accessible lipid concentration, taken as one-half the total lipid concentration since the peptides do not cross the bilayer. Because accessible [L] greatly exceeded bound peptide concentration, the peptide did not affect significantly the total surface charge.

EPR Spectroscopy and EPR Binding Data Analysis. EPR spectra (X-band) were recorded from ~5 μL samples using a Varian E-line century series spectrometer fitted with a MITEQ microwave amplifier and a two-loop one-gap resonator. Spectra were measured using a microwave power of ≤2 mW and a modulation of 1 G peak-to-peak. Peptides were added in steps from a concentrated stock solution to 100 μL of a 20 mM lipid vesicle suspension [0.25 mol % proxyl PI(4,5)P_2]. The first derivative peak-to-peak amplitude of the central nitroxide resonance, $A(0)$, was measured and plotted as a function of peptide concentration.

The association constant, K_a, for 1:1 binding of SCAMP E peptide to proxyl-PI(4,5)P_2 is given by

$$K_a = \frac{[M \cdot PIP_2]}{[M][PIP_2]} \quad (2)$$

where [M·PIP$_2$] represents the concentration of peptide−PI(4,5)P_2 complex, [PIP$_2$] is the concentration of free PI(4,5)P_2, and [M] is the concentration of macromolecule in aqueous solution (*25*). When $[M]_{total}$ and $[PIP_2]_{total}$ represent of total concentration of macromolecule and PI(4,5)P_2, respectively,

$$[M]_{total} = [M] + [M \cdot PIP_2] \quad (3)$$

$$[PIP_2]_{total} = [PIP_2] + [M \cdot PIP_2] \quad (4)$$

Therefore, the above three equations yield a quadratic expression that can be used to predict the binding as a function of peptide concentration. Since the EPR spectrum is a simple sum of EPR spectra from the free (non-peptide associated) and bound proxyl-PI(4,5)P_2, the central EPR resonance amplitude, $A(0)$, can be given as

$$A(0) = \frac{[PIP_2]}{[PIP_2]_{total}} A_f + \frac{[M \cdot PIP_2]}{[PIP_2]_{total}} A_b \quad (5)$$

where A_f and A_b represent the amplitudes of the central resonance obtained for free and bound proxyl-PI(4,5)P_2, respectively. In the present case, A_f and A_b were non-normalized amplitudes that were recorded under identical spectrometer settings. Values of K were determined by a nonlinear fit of $A(0)$ versus $[M]_{total}$, where K and A_b were adjustable parameters.

Bicelle Preparation and NMR Spectroscopy. A concentrated stock solution of dicaproylphosphatidylcholine (DCPC) in H_2O was prepared in a glove bag filled with dry N_2. The bicelle samples containing SCAMP E peptides were formed by mixing the appropriate amounts of dry dimyristoylphosphatidylcholine (DMPC), dimyristoylphosphatidylglycerol (DMPG), and different SCAMP E peptides with the DCPC solution, and NaCl in D_2O was added to 150 mM final concentration. The volume was adjusted with H_2O to 90% of final volume (~500 μL), pH was adjusted to 5.5, and the sample was then diluted to final volume. The mixture was subjected to five cycles of freeze−thaw, and pH was checked again. Samples contained 4 mM peptides, 150 mM NaCl, 15% (w/v) bicelles, 10% (v/v) D_2O, pH 5.5. The lipid content of the bicelles was 67 mol % DCPC, 20 mol % DMPG, and 13 mol % DMPC. Samples were degassed by freeze−pump−thaw (3−4 times) and then equilibrated with 9 atm of O_2 or N_2. NMR spectroscopy has been previously described (*25*).

Values of the oxygen-induced spin−lattice relaxation rate, R_{1para}, were determined as done previously (*25*, *27*), and the binding location of SCAMP E peptides were estimated by comparing R_{1para} values for the peptides with those of the bicelle lipids.

Cell Culture and Gene Expression. Rat pheochromocytoma PC12 cells (tet-off) were from BD Bioscience Clontech (used for assay of hGH secretion), and from Edwin Chapman (University of Wisconsin, Madison, WI; used for amperometry). Cells for human growth hormone (hGH) assay were cultured in DMEM containing 10% horse serum, 5% fetal bovine serum (BD Biosciences Clontech), and those for amperometry were cultured in DMEM containing 5% horse serum, 5% iron-supplemented calf serum (Hyclone Laboratories Logan, UT). Both types of cells were cultured at 10% CO_2, 37 °C. Tet-off PC12 cells were transfected with Lipofectamine Plus (*19*). Samples were incubated for different time periods before adding doxycycline (2 μg/mL) in order to achieve similar levels of overexpression of SCAMP2 variants; overexpression was judged by assaying the level of myc-SCAMP2 (relative to endogenous SCAMP2) by Western blotting and the fraction of transfected cells using immunofluorescence (*19*). PC12 cells used in amperometry were transfected by electroporation (single 7 ms pulse, 225 V, 2 mm cuvette; ECM830 electrosquare porator). Ten micrograms of DNA was used for 6×10^6 cells in 35 μL of electroporation buffer (*28*) per electroporation. Transfection conditions were the same as used previously, which results in expression of exogenous SCAMP2 constructs at ~5-fold above endogenous levels (*20*).

Human Growth Hormone (hGH) Secretion Assay. The assay for hGH secretion in cells cotransfected with DNAs encoding hGH and SCAMP2 variants was carried out as described previously (*19*, *29*). Briefly, the cells were washed with low-K^+ buffer (5.6 mM glucose, 5.6 mM KCl, 145 mM NaCl, 2.2 mM $CaCl_2$, 0.5 mM $MgCl_2$, 15 mM HEPES, pH 7.4) at 72 h after transfection and then incubated in succession with low-K^+ buffer and high-K^+ buffer (5.6 mM glucose, 56 mM KCl, 95 mM NaCl, 2.2 mM $CaCl_2$, 0.5 mM $MgCl_2$, 15 mM HEPES, pH 7.4), at 37 °C (10 min each incubation). After incubation, the media and the cell lysates were used for assay of hGH by ELISA; secretion is presented as percentage of total hGH (± standard error, 4 assays).

Amperometry. PC12 cells transfected with pIRES-EGFP constructs were cultured on poly-D-lysine/collagen (5 μg/cm^2 of each)-coated 35 mm dishes for 44 h. The cells were loaded with 1.25 mM NA, 0.25 mM ascorbate in medium for 12−16 h. After loading and 1−3 h chase in culture medium, cells were transferred to the buffer containing 142 mM NaCl, 4.2 mM KCl, 1 mM Na_2HPO_4, 0.7 mM $MgCl_2$, 2 mM $CaCl_2$, and 10 mM HEPES, pH 7.3. Cells expressing GFP were selected and stimulated by local perfusion (3 psi from an Eppendorf Transjector 5246) of K^+ depolarizing medium (105 mM KCl, 45 mM NaCl, 1 mM NaH_2PO_4, 0.7 mM $MgCl_2$, 2 mM $CaCl_2$, and 10 mM HEPES, pH 7.3) from a 2 μm diameter micropipet placed ~10 μm away from the

cell surface. Release of NA was detected by a cut 5 μm carbon fiber lightly contacting the cell surface and at a potential of +660 mV. Current signals were fed to an Axopatch 200 amplifier, low-pass filtered at 1 kHz and digitized at 3.3 kHz by a computer running Lab Man (a custom data acquisition program developed in the Szabo laboratory). Each cell was stimulated for 8 s at 30 s intervals with K^+ depolarizing medium.

Individual experiments were performed on cells transfected with pIRES2-EGFP vector, mutant SCAMP2 constructs. The morphology of all types of cells recorded was indistinguishable. Thus contributions of small spikes that reflect increased distance from the electrode to recordings are anticipated to be comparable in all samples. Recordings were analyzed using computer programs provided by Meyer Jackson and Payne Chang (University of Wisconsin). The current signals with amplitudes exceeding five times the background noise ($\sim$ 0.3−0.4 pA) were counted as exocytotic events. Once identified, events with peak amplitude $\geq$4 pA having sharp upward/downward deflections were designated as spikes; while the smaller events with amplitudes comparable to those of the foot currents of spikes ($\sim$2 pA) were identified as stand-alone-feet (SAF) (*20*, *30*). The prespike feet (PSF) with duration $\geq$1 ms (3 times the data sampling rate to minimize inaccurate measurements) from big spikes (>8 pA) were analyzed; lifetime distributions of PSF were plotted and fitted to exponentials using the Origin program (MicroCal Software, Northampton, MA) (*20*, *28*). To control for cell-to-cell variability in secretory response, results were calculated as means for all cells in an experimental sample (>40 cells per group from multiple transfections for each protein) (*31*, *32*). Ratios of SAF/spikes were calculated as the slope of linear fits to plots of number of SAF versus number of spikes. All results are reported as means ± SEM, and one-way analysis of variance (ANOVA) was used to evaluate statistical significance.

RESULTS

Binding of SCAMP E Peptide to PI(4,5)P_2-Containing Lipid Vesicles Depends on Specific Amino Acid Residues. Our previous work indicated that the peptide lacking tryptophan (W2) loses its potency as an inhibitor of exocytosis in permeabilized cells while the W202A mutant of full-length SCAMP2 strongly inhibits exocytosis when expressed in PC12 cells (*18*−*20*). Because the E peptide segment of full-length SCAMP2 is constrained to locations that are at least near to the membrane surface by flanking transmembrane spans, we have been interested in evaluating how peptide positioning might affect protein function. To begin to address this issue, we have focused on membrane binding and lipid interactions of synthetic peptide variants in which W2, R4, and K8 have been replaced individually. For W2 and R4, alanine substitutions were made; in the case of K8, we chose to use a natural variant, the SCAMP1 E peptide (CWYRPLYGAFR), not only to examine the consequences of K replacement but also to detect potential distinct properties for the two SCAMP isoforms. To measure membrane-binding affinities for the peptides (as well as unsubstituted SCAMP2 E peptide as a control), we used a vesicle sedimentation assay (*24*, *25*). However, instead of monitoring the distributions of peptides derivatized with ^{3}H-NEM, we assayed the underivatized cysteinyl sulfhydryls spectrophotometrically (see Materials and Methods). Vesicles used for binding were composed of PC/PS/PI(4,5)P_2 (79.9:20:0.1), and the plots of the fraction of peptide bound as a function of the concentration of accessible lipid are shown in Figure 1. The association constant, *K*, of SCAMP2 E peptide is 1.25 × 10^3 M^{-1}, which falls between the *K* values measured previously (0.89 × 10^3 M^{-1} and 1.4 × 10^4 M^{-1}), using vesicles containing PC and either 1 or 3 mol % PIP_2, respectively (*25*). Thus observed binding is consistent with the nonspecific Coulombic interaction of the peptides with the negatively charged membrane surface (*25*). For SCAMP1 E peptide, the measured *K* of 1.5 × 10^3 M^{-1} is very similar to that of SCAMP2 E peptide. Thus the K8 residue does not figure significantly in binding, and it appears that naturally occurring SCAMP E peptides generally associate with the negatively charged membranes with about the same efficiency. Interestingly, the *K* of the R4A substitution of SCAMP2 E peptide, 2.94 × 10^3 M^{-1}, is about 2-fold higher than the *K*'s for the naturally occurring E peptides. The slightly increased binding for SCAMP2-R4A E peptide is unexpected due to the reduced positive peptide charge, but may reflect a reduced energy penalty that accompanies positioning a basic residue within the low dielectric membrane interface. Notably, SCAMP2-W2A E peptide has a dramatically lower *K*, 36.1 M^{-1}, which is 35-fold smaller than that of SCAMP2 E peptide (SC2-WT). This change correlates quite well with previous findings that the free energy of transfer for tryptophan from an organic solvent to water is $\sim$2.5 kcal/mol larger than that for alanine (*33*), which is predicted to result in $\sim$50-fold difference in the partition coefficient. Evidently, SCAMP2-W2A E peptide is deficient in membrane binding, which might signify a reduced tendency or capability of this segment of the full-length protein to insert into the membrane interface.

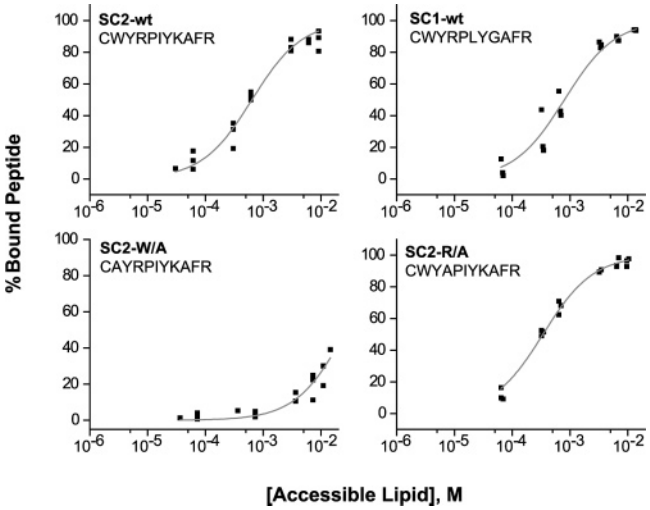

FIGURE 1: Binding of SCAMP (SC) E peptides to sucrose-loaded membrane vesicles [PC/PS/PI(4,5)P_2 = 79.9:20:0.1] as a function of the concentration of accessible lipid. Peptide concentrations are 10 μM. Percentage of bound peptide has been deduced by centrifugation and spectrophotometric assay of nonsedimentable (cysteine-containing) peptide. The curves are calculated from the data using eq 1. The molar partition coefficients are 1.25 × 10^3 M^{-1}, 1.50 × 10^3 M^{-1}, 2.94 × 10^3 M^{-1}, and 3.61 × 10^1 M^{-1} for SC2-WT (wild type), SC1-WT, SC2-R4A, and SC2-W2A E peptides, respectively.

Arginine R4 but Not Lysine K8 Is Critical for the Binding of SCAMP E Peptides to Proxyl-PI(4,5)P_2. Electrostatic

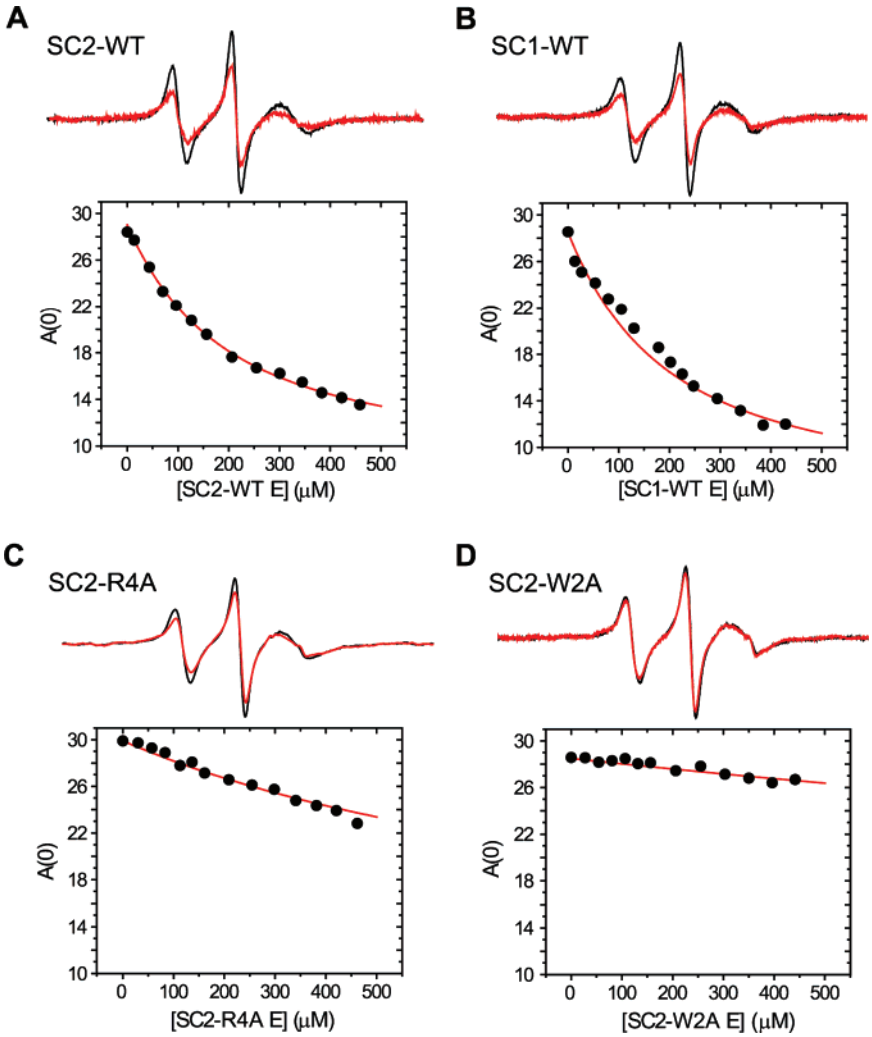

FIGURE 2: Sequestration of PI(4,5)P_2 by SCAMP (SC) E peptides detected by EPR spectrometry of proxyl-PI(4,5)P_2. Examples of EPR spectra of proxyl- PI(4,5)P_2 in the absence (black traces) and presence (red traces) of ~0.5 mM of SC2-WT (A), SC1-WT (B), SC2-R4A (C), and SC2-W2A (D) E peptides are in the upper parts of panels A−D. Titrations of the central EPR resonance of proxyl-PI(4,5)P_2 as a function of the concentration of added SCAMP E peptides are shown under the EPR spectra in A−D, respectively. The EPR spectra are 100 G scans. The red solid lines represent nonlinear least-squares fits of the data using eqs 2−5 (Materials and Methods).

interactions between peptides enriched in basic and aromatic residues and PI(4,5)P_2 could be demonstrated clearly by examining EPR spectra of spin-labeled (proxyl) PI(4,5)P_2 incorporated into PC liposomes (*25*, *34*). In particular, addition of SCAMP2 E peptide to these liposomes caused dose-dependent spectral broadening and decreased amplitude, which was readily detected from the central resonance. The change in the EPR spectrum produced by addition of the peptide represents a 0.5 to 1 ns increase in the correlation time of the nitroxide that is likely due to a change in rotational diffusion rate about the long axis of the spin-labeled PI(4,5)P_2 and indicative of an interaction with the peptide (*25*). Because our substitutions in SCAMP2 E peptide involved basic and aromatic residues, we sought to compare their effects to that of normal E peptide on proxyl-PI(4,5)-P_2-containing liposomes. Figure 2 shows representative spectra from each type of sample and presents plots of the central resonance amplitude as a function of concentration of peptide added. In order to estimate values of K_a, all plots were fitted by nonlinear least-squares using the 1:1 binding model (Table 1). The results show that SCAMP1 and SCAMP2 E peptides (SC1-WT and SC2-WT) bind proxyl-PI(4,5)P_2 with a similar affinity (K_a ~5 × 10^3 M^{-1}). Thus, the K8 residue of E peptide does not detectably participate in PI(4,5)P_2 interaction in addition to its lack of participation in vesicle binding. In contrast, SCAMP2-R4A E peptide exhibits a much weaker affinity (K_a ~ 800 M^{-1}) to PI(4,5)-P_2 even though its binding to negatively charged lipid membranes is 2-fold higher than for both of the naturally occurring E peptides. This outcome indicates that the R4 residue is critical for the electrostatic interaction between peptide and PI(4,5)P_2. Although not addressed, it is likely

Table 1: K_a Values Derived from EPR Experiments[a]

	sequence	K_a (M^{-1})
SC2-WT	CWYRPIYKAFR	5000
SC1-WT	CWYRPLYGAFR	5000
SC2-R4A	CWYAPIYKAFR	800
SC2-W2A	CAYRPIYKAFR	200

[a] The values derived from fitting eqs 2−5 to the amplitude changes in the EPR spectrum of proxyl PI(4,5)P_2 (Figure 2). The errors in the estimated values of K_a are approximately ±30% or less. This estimate of error is based upon the maximum standard deviations that are obtained when repetitive titration measurements are made and then fitted using the procedures described here (see Materials and Methods).

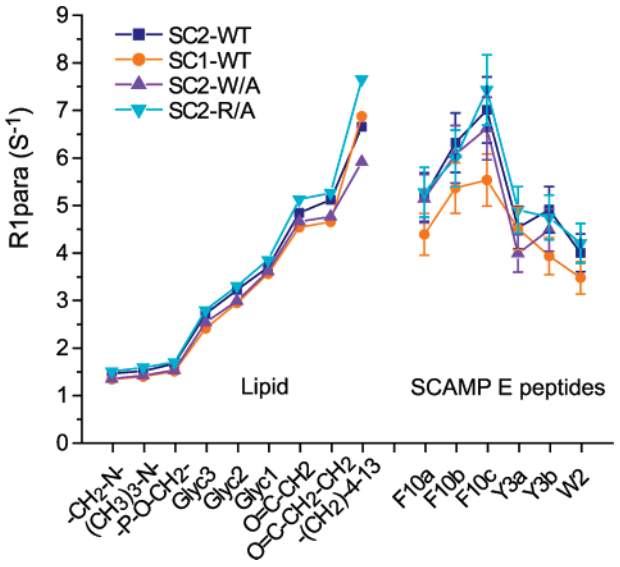

FIGURE 3: Oxygen-induced spin−lattice relaxation rates (R_{1para}) in units of s^{-1} for several bilayer lipid and peptide ^1H resonances from bicelles bound with different SCAMP (SC) E peptides, including SC2-WT (■), SC1-WT (●), SC2-R4A (▲), and SC2-W2A (▼) E peptides. The vales of R_{1para} were measured and calculated as described in Materials and Methods; values reflect oxygen solubility within the hydrocarbon and vary as a function of depth within a lipid bicelle. Individual lipid resonances are arranged in order to increasing distance (left to right) from the membrane surface. Errors were derived from exponential fitting of oxygen relaxation curves.

that R11, which is located at a similar depth within the membrane as R4 (*25*), is also critical for the interaction. Addition of SCAMP2-W2A E peptide did not alter the EPR spectrum of proxyl-PI(4,5)P_2. This result is not surprising because the concentration of proxyl-PI(4,5)P_2-containing lipid membranes (~25 mM) is too low for sufficient binding of the peptide lacking tryptophan (Figure 1).

Interfacial Locations of SCAMP E Peptides Determined by NMR. We were interested to examine how the differences among the peptides in their abilities to interact with PI(4,5)P_2 related to their interfacial locations within lipid membranes. Therefore, we employed NMR, capitalizing on previous proton chemical shift assignments for unsubstituted SCAMP2 E peptide bound to bicelles (*25*), and measured proton spin−lattice relaxation rates for bicelle-bound peptides in the absence and presence of oxygen. For reference, the resonance assignments for SCAMP E peptide in solution and in bicelles are included as Supporting Information. The paramagnetic enhancements of proton spin−lattice relaxation rate due to oxygen, R_{1para}, for lipid and peptide protons have been aligned for all types of samples and are shown in Figure 3. As expected from previous findings, the values of R_{1para} for bilayer lipid protons progressively increase proceeding from the choline methyls of the PC headgroup toward the methyl termini of the fatty acid chains, reflecting increased solubility of O_2 in the membrane hydrocarbon phase (*25*, *35*).[2] Based on the lipid calibration, the unsubstituted SCAMP2 E peptide was positioned almost exactly as measured previously (*25*), with its backbone nearly coincident with the glycerol segment of the phospholipids in the bilayer interface. Most of the aromatic side chains reach the lipid hydrocarbon. Since the values of R_{1para} for the lipid protons were very consistent among the different preparations, the values of R_{1para} for the peptide protons were compared directly. Surprisingly, no significant differences were observed for the locations of aromatic side chains from different E peptides except that the interfacial location of SCAMP1 E peptide (SC1-WT) is slightly closer to the membrane surface (Figure 3). Thus SCAMP2-R4A E peptide has the same position as the unsubstituted peptide even though it binds to vesicles with higher affinity, and the loss of PI(4,5)P_2 interaction is strictly related to the removal of the arginine residue. In the case of SCAMP2-W2A E peptide, the very high lipid concentration employed in the bicelle preparations forces binding, and it is striking that the peptide achieves the same depth in the interface as unsubstituted peptide. Because tryptophan is unlikely to play a direct role in PI(4,5)P_2 binding, it may function solely to drive the basic residues to a depth where they will bind the polyvalent lipid. However in physiological conditions, insufficient binding to the membrane may be a significant issue for the E peptide segment of full-length SCAMP2-W202A.

Perturbation of Neuroendocrine Secretion by E Peptide Mutants of SCAMP2. The results demonstrating distinct membrane binding and PI(4,5)P_2 interaction properties of SCAMP E peptides and the single amino acid variants seemed potentially insightful with respect to understanding our earlier findings regarding the role of SCAMPs in DCV exocytosis and possible connection to the function of PI(4,5)P_2 in the process. In those studies, we showed that E peptide's potency as an inhibitor of exocytosis in permeabilized cells was nearly abolished by substituting alanine for the aromatic residues and that the W202A mutant of SCAMP2 was a powerful and dose-dependent inhibitor of secretion when expressed in PC12 cells (*18*, *19*). Thus we examined mutations involving arginine and lysine residues with the goal of determining if the effects on DCV exocytosis were similar or distinct from those of the tryptophan mutation. Myc-tagged SCAMP2-R204A and K208A were expressed in PC12 cells in parallel with wild-type SCAMP2, SCAMP2-W202A, or empty vector. Note that, in contrast to the peptide studies above, SCAMP2-K208A was used in lieu of SCAMP1 to introduce only a single variable in the experiments. To screen for inhibitory effects on secretion, the cells were cotransfected with human growth hormone (hGH) and were tested for both unstimulated and depolarization-induced hGH secretion (*19*). We also evaluated the level of expression of the myc-tagged constructs by Western blotting and their intracellular distributions by immunofluorescence performed on both intact cells and plasma membrane lawns (*19*). In all cases, the exogenous SCAMPs were expressed at a level corresponding to 4-fold higher than endogenous SCAMP2. Further, they distributed quite similarly to the endogenous SCAMP (data not shown). Effects of the exogenous SCAMPs on hGH secretion are shown in

[2] Earlier work (*25*) assigned the resonances for the two arginine residues in the E peptide and placed these deep within the bicelle interface. However, examination of the NMR spectrum from the mutant peptide, W2A, indicates that the previous assignment of the arginine side chain guanidino protons is incorrect and consequently the location of these atoms is less certain than previously stated. However the previous and current data (see Results) puts all resolvable backbone amide protons (>75% of all backbone amides) at the level of the lipid glycerol protons. Therefore while the R guanidino protons may not be located as close to the lipid hydrocarbon region of the bilayer as previously suggested, they must be within or very close to the bilayer interfacial region.

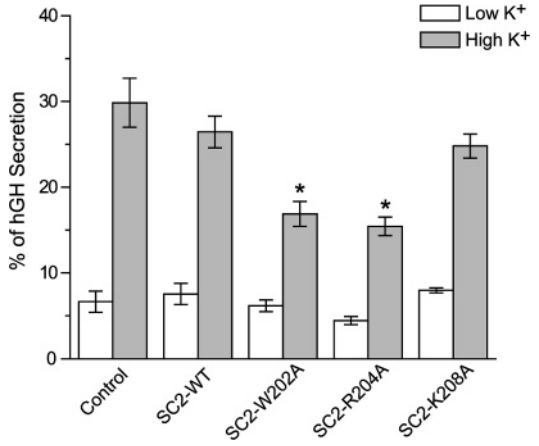

FIGURE 4: Expression of SCAMP2 and its mutants in PC12 cells and effects on depolarization-induced secretion of human growth hormone (hGH). PC12 cells were cotransfected with cDNAs encoding hGH and either pTRE2 vector (control), myc-tagged wild-type SCAMP2, mutant W202A, R204A, or K208A, and then treated with 2 μg/mL doxycycline (dox) at times that achieve comparable levels of expression. At 72 h after transfection, the cells were incubated 10 min in low-K^+ buffer; depolarization (10 min) was then initiated by replacing the medium with high-K^+ buffer. Media and cell lysates were assayed for hGH by ELISA. Results are expressed as % total hGH and are averaged from four independent experiments (mean ± SEM). * indicates $p < 0.01$ as compared to control samples for the same experimental conditions.

Figure 4. Consistent with previous results (*19*), overexpression of SC2-WT had little effect on stimulated hGH secretion. SC2-R204A inhibited secretion to a similar extent as SC2-W202A; both were significantly different from SC2-WT whereas SC2-K208A was not. Interestingly, these distinctions in capacity to inhibit DCV exocytosis parallel the distinctions observed for E peptide binding to PI(4,5)P_2 (Figure 2), although in the latter case, arginine and tryptophan substitutions probably abrogate PI(4,5)P_2 binding for different reasons, as discussed above.

Exogenous Expression of SCAMP2-R204A Affects the Rate of Membrane Fusion and Fusion Pore Stability. As indicated in the introduction, we have shown that expression of SCAMP2-W202A perturbs both early and late events during exocytosis of DCVs (*20*). These effects were distinguished using amperometry to monitor secretion, which has millisecond resolution and is able to provide detailed information about the kinetics of NA release from fusion pores. Therefore, we pursued the prospective correlation between E peptide − membrane and PI(4,5)P_2 interaction and effects of SCAMP2 mutants on secretion by amperometry analysis from PC12 cells expressing the SCAMP2 mutants R204A and K208A. Cells were transfected with SCAMP2 constructs using a bicistronic GFP-containing vector enabling identification of transfected cells by fluorescence; transfection with the same vector containing GFP alone was used as control. Transfection conditions were the same as used previously, which results in expression of exogenous SCAMP2 constructs at ~5-fold above endogenous levels (*20*). Representative recordings obtained from the three types of cells resulting from 8 s depolarization by local perfusion of 105 mM KCl are shown in Figure 5A. The exocytotic signals were recognized when the current rose 5-fold above background noise (~0.3−0.4 pA). In contrast to the control, very few events are detected in the traces from cells expressing SCAMP2-R204 (Figure 5A); in fact, ~50% of cells that were tested exhibited no detectable response. This indicates a potent inhibition of NA secretion that appears even stronger than observed previously for SCAMP2-W202A (*20*). In the case of cells expressing SCAMP2-K208, the responses appear slightly decreased relative to the control, suggesting a mild inhibitory effect on exocytosis (Figure 5A). To analyze effects on the fusion pore opening, we followed a previous strategy (*20*, *36*) and plotted the cumulative appearance of exocytotic events averaged from all recordings for each type of cells as a function of time (Figure 5B). The frequencies of fusion pore opening were measured as the initial slope of the curves and were plotted in Figure 5C; the maximum release after depolarization (total number of exocytotic events calculated at 30 s after stimulation) reflects the size of the releasable vesicle pool and is shown in Figure 5D. Expression of SC2-R204A strongly decreases both the rate of membrane fusion and the size of the releasable vesicle pool; in fact, the values shown are likely to be overestimates because only responsive cells were included in the cumulative plot. In contrast, the inhibitory effect of SC2-K208A, while significant, is less extensive. For overall comparison, the mean values of amperometry parameters from each type of cells are listed in Table 2, including the data for wild-type SCAMP2 (SC2-WT) and SC2-W202A that were previously published (*20*) and reprocessed in the same way here for comparison. Both SC2-W202A and SC2-R204A substantially decreased the frequency of exocytosis to 26% and 11% of control, respectively; whereas SC2-K208A and SC2-WT decreased the frequency less extensively (53% and 80%, respectively). Table 2 also shows that SC2-R204A had a more profound inhibitory effect on the size of the releasable pool of DCVs than either SC2-W202A or SC2-K208A. These findings identify an interesting inverse correlation between the extent of E peptide association with PI(4,5)P_2 and the extent of inhibition of DCV exocytosis by overexpressing corresponding variants of SCAMP2.

Amperometry also resolves limited release of NA from the initially opened fusion pores before their dilation, as signified by the prespike foot (PSF) that precedes spike signals. The duration of the PSF is an index for the stability of initially opened fusion pores (*28*). We compared the PSF duration of large spikes for each type of cell and found that those expressing SC2-R204A but not SC2-K208A exhibited a decreased PSF duration (Figure 5E). The results led us to propose that the regulation of PI(4,5)P_2 level could indeed affect the properties of fusion pores, and it is possible that the change in PSF duration in cells expressing SC2-R204A is a reflection of inefficient association of this SCAMP2 mutant with PI(4,5)P_2.

In our previous study, we also compared the incidence of two types of exocytotic events—small stand-alone feet (SAF) and large spikes—between cells expressing different variants of SCAMP2 and also Arf6 (*20*). The SAF with current amplitudes at the level of PSF result from fusion pore opening and closure without dilation whereas spikes are indicative of pore dilation following opening (*30*). The averaged ratio of SAF to spikes from individual cells reflects the tendency of initially opened fusion pores to close rather than to dilate (*20*, *28*). We showed that SC2-W202A substantially increased the SAF/spike ratio (~3-fold; Table 2). Here we found that expression of SC2-R204A increased

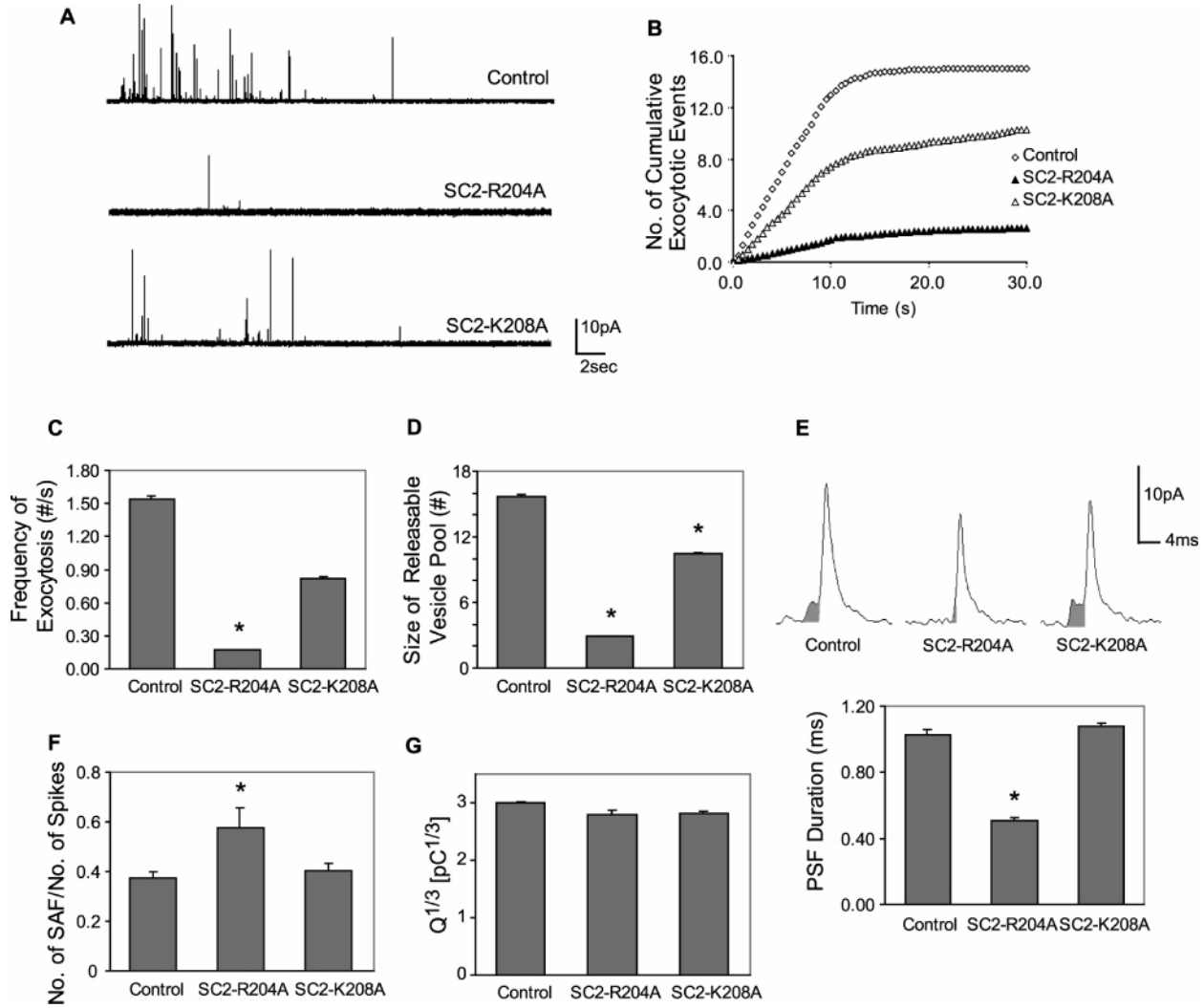

FIGURE 5: Effects of SCAMP2-R204A (SC2-R204A) and SCAMP2-K208A (SC2-K208A) on NA secretion by PC12 cells analyzed by amperometry. (A) Representative recordings of PC12 cells transfected with pIRES2-EGFP vector (control), SCAMP2-R204A (SC2-R204A), and SCAMP2-K208A (SC2-K208A). Depolarization (105 mM K^+) was for the first 8 s, and the length of each record was 30 s. Each construct was transfected into cells in 3−4 independent experiments. (B) Plots of cumulative exocytotic events over 30 s in each type of sample calculated from the means of samples (51 cells for control, 62 cells for SC2-R204A, and 58 cells for SC2-K208A). (C) Mean frequency of exocytosis calculated as the initial slope from the plots in (B). (D) The sizes of the releasable vesicle pool calculated as the maximum level of release 30 s after depolarization averaged over all cells in each sample. The frequency of membrane fusion for cells expressing SC2-R204A is too low to quantitate standard error of the mean (SEM). (E) The shaded regions indicating the prespike foot signals determined by the baseline and spike onset. The mean open time of prespike feet was obtained from single-exponential fits of the distribution of PSF lifetimes and is plotted in the lower panel. Number of spikes analyzed for control = 150, SC2-R204A = 53, SC2-K208A = 190. (F) SAF/spikes ratio shown as a bar graph; values are slopes of best-fit lines for scatter plots of number of SAF versus number of spikes. The types of exocytotic events are distinguished by shape and amplitude (see Materials and Methods). (G) Bar graph of mean values of the cubic root of quantal size of spikes. All results are mean ± SEM, and one-way ANOVA was used to evaluate statistical significance; * indicates $p < 0.01$.

the ratio less than 2-fold whereas SC2-K208A had no effect (Figure 5F and Table 1). The observations that SC2-W202A substantially increases the SAF/spike ratio but does not alter PSF duration whereas SC2-R204A only moderately increases the SAF/spike ratio but significantly decreases PSF duration raise the possibility that SC2-W202A and SC2-R204A inhibit fusion pore dilation through different mechanisms.

As a part of our study, we also quantitated the charge associated with oxidation of NA detected as current spikes. Since the cube root of total charge has a Gaussian distribution (*37*), we calculated the mean value of the cube root of spike areas. In contrast to SC2-W202A, which decreased the mean value significantly (*20*), SC2-R204A and SC2-K208A had no effects on the quantal size of NA release (Figure 5G and Table 2).

DISCUSSION

We have brought together two themes that have emerged in efforts to understand the function and regulation of PI(4,5)P_2 at the plasma membrane in controlling exocytosis and to address how SCAMP2 might participate in these processes. First, physical chemical studies have shown that various proteins are able to regulate PI(4,5)P_2 by electrostatic association; the resulting concentration of these polyanionic lipids may either restrict or potentiate function at specific sites on the cell surface (*38*). Second, cell biological studies have highlighted biosynthesis of PI(4,5)P_2 and its involvement in generating scaffolds that organize membrane trafficking events (*1*). We have focused on the E peptide segment of SCAMP2, which exhibits the basic and aromatic amino

Table 2: Values of Amperometric Parameters[a]

	control ($n = 51$)		SC2-R204A ($n = 62$)		SC2-K208A ($n = 58$)	
	mean	±SEM	mean	±SEM	mean	±SEM
size of releasable vesicle pool (no.)	15.67	±0.15	2.90	±0.04	10.97	±0.11
frequency of exocytosis (no./s)	1.54	±0.03	0.17	?	0.82	±0.02
prespike foot duration (ms)	1.03	±0.03	0.51	±0.01	1.08	±0.02
ratio of SAF/spikes	0.38	±0.02	0.58	±0.08	0.41	±0.01
spike size$^{(1/3)}$ [pC$^{(1/3)}$]	2.91	±0.03	2.80	±0.07	2.81	±0.04
	control ($n = 66$)		SC2-WT ($n = 49$)		SC2-W202A ($n = 54$)	
	mean	±SEM	mean	±SEM	mean	±SEM
size of releasable vesicle pool (no.)	18.23	±0.27	19.29	±0.53	8.70	±0.37
frequency of exocytosis (no./s)	1.11	±0.02	0.89	±0.02	0.29	±0.01
prespike foot duration (ms)	1.05	±0.02	0.95	±0.01	1.02	±0.03
ratio of SAF/spikes	0.37	±0.03	0.37	±0.04	1.11	±0.13
spike size$^{(1/3)}$ [pC$^{(1/3)}$]	2.38	±0.04	2.37	±0.03	1.80	±0.04

[a] The values measured in amperometry study for depolarization-induced DCV exocytosis using PC12 cells transfected with pIRES2-EGFP vector (control), SCAMP2 mutants SC2-R204A and SC2-K208A (upper panel). The data for SC2-WT and SC2-W202A obtained from our previous study (*20*) were processed in the same way for comparison (lower panel).

acid composition characteristic of proteins that electrostatically sequester PI(4,5)P_2 and at the same time has been implicated in early and late events in exocytotic fusion that may involve the synthesis and binding of PI(4,5)P_2 (*20*, *25*).

Building on our previous findings that synthetic E peptide, which constitutes most of the oligopeptide segment linking the second and third transmembrane spans of full-length SCAMP, binds to membranes deep within the interface and sequesters PI(4,5)P_2 by a 1:1 electrostatic association (*25*), we have now examined variants of E peptide that incorporate specific amino acid replacements. We focused on residues having the strongest possibility for evaluating the prospective relationship between PI(4,5)P_2 interaction and function in exocytosis: W2, an established exocytotic inhibitor as SCAMP2-W202A; R4, a putative key component of PI(4,5)P_2 binding; and K8, a basic residue "control" not anticipated to influence PI(4,5)P_2 binding. Investigation of K8 also facilitated prediction of PI(4,5)P_2 interaction with SCAMP1, because change of K to G is the only significant difference between E peptide segments of the two SCAMP isoforms. Our results revealed distinct characteristics in each case when compared to the naturally occurring E peptide of SCAMP2. The W2A substitution uniquely and strongly reduced peptide binding to membranes; the R4A substitution slightly increased binding but abrogated interaction with proxyl-PI(4,5)P_2; and the K8A substitution (SCAMP1 E peptide) affected neither binding nor proxyl-PI(4,5)P_2 interaction. With regard to the R4A substitution, the increased membrane binding but loss of PI(4,5)P_2 binding might seem counterintuitive; however, we would argue that the findings are compatible because these interactions are thought to be driven by different intermolecular forces. Previous experimental (*39*) and computational work (*40*) has shown that the binding free energy of charged peptides to negatively charged membranes is determined by a balance of a long-range Coulombic attraction and a short-range dehydration (repulsive) interaction. Because of this dehydration force, placement of a charged amino acid side chain at or within the bilayer interface is energetically unfavorable, relative to positioning the side chain a few angstroms on the aqueous side of the membrane interface. In the case of the SCAMP E peptide, we speculate that the aromatic residues act to position the charged residues within the bilayer interface, in a manner similar to that seen previously for the effector domain of MARCKS (*39*). According to this reasoning, the R4A E peptide mutant should bind with a similar (or slightly stronger) affinity than the wt peptide because binding is largely driven by hydrophobic interactions. The free energy contributed by the Coulombic attraction of R4 in the wt peptide to the negatively charged membrane interface is largely offset by the energy expended in burying this side chain within the interface. Reduced positive charge, particularly within the interface, is known to be associated with a reduction in the sequestration of PI(4,5)P_2 (*41*), which provides a plausible explanation for the reduction in PI(4,5)P_2 sequestration by the R4A mutant peptide (and potentially by full-length R204A mutant SCAMP2).

Interestingly, positional analysis by NMR under conditions where all peptides were membrane bound indicated that the four peptides were situated quite similarly with aromatic residues extending into the nonpolar membrane interior occupied by phospholipid methylene groups. While the poor membrane binding of the W2A E peptide precluded evaluation of its association with proxyl-PI(4,5)P_2, we suspect that unstable membrane binding and thus reduced tendency to insert deep into the surface could be a significant factor affecting such an association since tryptophan is not known to figure specifically in PI(4,5)P_2 interaction. Collectively, these studies point to a range of peptide−PI(4,5)P_2 associations: 1:1 binding for naturally occurring SCAMP2 E peptide (sufficiently stable to block phospholipase C-mediated cleavage of the lipid (*25*)); comparable interaction following K8A substitution; compromised interaction following W2A substitution due to unstable membrane binding; and abrogation of interaction upon R4A substitution.

Our analysis of DCV exocytosis in PC12 cells overexpressing SCAMP2 and point mutations showed striking correlation with the trend established for the interaction of the peptides with PI(4,5)P_2. Expression of SCAMP2s W202A and R204A involving E peptide residues that are critical for PI(4,5)P_2 association profoundly inhibited exocytosis (*20*) whereas expression of normal SCAMP2 or a K208A mutant had at most a minor inhibitory effect. To legitimize pursuit of this correlation, we previously showed that endogenous and exogenous SCAMP2s and mutants are concentrated close to presumptive exocytotic sites where DCVs are docked and

that the inhibitory effects of the mutants are manifest at the plasma membrane (*19*, *20*). In all cases, direct effects of the exogenous SCAMPs on DCVs, for example on their formation in the TGN and their loading with NA prior to analysis of exocytosis, seem quite unlikely because the incidence and localization of DCVs are not altered (data not shown) and SCAMP2 does not reside in DCVs (*19*). Examination of the effects of expression of SCAMP2 and its mutants on secretion of cotransfected hGH clearly distinguished wild-type SCAMP2 and SCAMP2-K208A from SCAMP2-W202A and SCAMP2-R204A, i.e., the putative $PI(4,5)P_2$ interaction-competent and incompetent forms. However, the increased resolution afforded by amperometry revealed distinct and potentially insightful perturbations of DCV exocytosis by each of the mutants. SCAMP2-K208 decreased the frequency of exocytosis beyond the minor inhibition caused by SCAMP2-WT but did not detectably affect the dynamics of nascent fusion pores (see Table 2). Thus effects of this mutant appear restricted to events preceding fusion. For SCAMP2-W202A, we showed previously that its expression significantly depressed the rate of fusion pore opening and the maximum number of observable events, prolonged the lag in onset of response, and destabilized open fusion pores such that they tended to close rather than dilate (*20*). For SCAMP2-R204A, inhibition of exocytosis was so profound that we could not reliably resolve effects on the different parameters used to evaluate events leading to fusion pore opening, although we feel reasonably confident in suggesting that these effects are even stronger than in the case of SCAMP2-W202A. Notably, for SCAMP2-R204A we also observed a substantial and unique reduction in prespike foot duration (Figure 5) signifying destabilization of opened fusion pores in a manner that is distinct from destabilization caused by the W202A mutant.

How might interactions of SCAMP2 with $PI(4,5)P_2$ be involved in these effects and reflect the role of $PI(4,5)P_2$ in DCV exocytosis? Associations of SCAMP2 with plasmalemmal machinery involved in $PI(4,5)P_2$ biosynthesis place SCAMP2 at the source of $PI(4,5)P_2$ that is produced to support exocytosis (*20*). However, the concentration of SCAMPs in clusters and potential multimerization (*15*, *42*, *43*) raise the possibility that SCAMP2 might also contribute to maintaining $PI(4,5)P_2$-enriched microdomains that accumulate at exocytotic sites (*13*). More specifically, since the mutants of SCAMP2 suspected to be defective in $PI(4,5)P_2$ interaction profoundly inhibit events preceding fusion pore opening, the SCAMP2 association with $PI(4,5)P_2$ might directly affect these upstream events. In particular, the interaction may regulate priming of the exocytotic machinery for the following reasons: the majority of DCVs in PC12 cells are docked but not primed (*44*, *45*); knockout of PI4P5K-1γ, the principal source of $PI(4,5)P_2$ for neuroendocrine exocytosis, does not affect docking (*11*); production of $PI(4,5)P_2$ has been linked to priming (*7*); and elevation of $PI(4,5)P_2$ increases the rapidly releasable pool of docked vesicles (*8*).

In addition to the possible role of $PI(4,5)P_2$−SCAMP2 interaction in priming, the correlation between reduced $PI(4,5)P_2$−E peptide interaction upon W2A and R4A substitutions and perturbation of fusion pore dynamics downstream of priming by SCAMP2s W202A and R204A suggest that $PI(4,5)P_2$−SCAMP2 interaction may figure importantly in regulating fusion pore formation. Formation of fusion pores involves changes in membrane curvature both during opening and during subsequent dilation. If interaction of $PI(4,5)P_2$ with SCAMP2 entails insertion of the E peptide segment into the membrane interface, this action could generate curvature stress in the bilayer, particularly if multiple locally concentrated SCAMP2 polypeptides participate in the process. Inability of mutant SCAMPs to stably associate with $PI(4,5)P_2$ (SCAMP2-W202A) or to bind $PI(4,5)P_2$ at all (SCAMP2-R204A) could underlie the destabilization of fusion pores that was detected by amperometry. Further, the stronger inhibition of exocytosis by SCAMP2-R204A than by W202A could reflect the difference between inability to bind versus unstable association with $PI(4,5)P_2$. In view of these suggestions, it seems quite interesting that binding of synaptotagmin's C2B domain to $PI(4,5)P_2$ within the cytoplasmic interface of the plasma membrane of neuroendocrine cells is thought to contribute to regulating fusion pore dynamics during DCV exocytosis and that overexpression of synaptotagmin alters the prespike foot duration (*10*, *28*). Thus, as noted previously, SCAMP2 and synaptotagmin may cooperate in regulating fusion pore formation, and multiple proteins may interact with $PI(4,5)P_2$ as a part of this role.

The striking sequence conservation of E peptide, both among mammalian SCAMP isoforms and evolutionarily, would seem to implicate this segment in a highly specific interaction. Yet the electrostatic association of SCAMP2 with $PI(4,5)P_2$ that we have addressed in this study emphasizes an interaction that requires less structural specificity. Indeed, we previously showed that rearrangement of residues within the E peptide did not alter the ability of the peptide to interact with $PI(4,5)P_2$ (*25*). Can these distinctions be rationalized? We are optimistic that they can and are interested in the possibility that the SCAMP2 E peptide may act at two levels. First, in supporting upstream events in DCV exocytosis, sequence-specific interactions of E peptide are likely to be involved in scaffolding the $PI(4,5)P_2$ biosynthetic machinery including activation of PLD1 (*20*). Early inhibitory effects on exocytosis, e.g., by SCAMP2-K208A (Figure 5) are consistent with this possibility, and highly specific interactions could involve other events related to priming. Second, downstream events controlling fusion pore formation would require electrostatic association of $PI(4,5)P_2$ with the E peptide segment of SCAMP2. We suggest that there may be coupling between the two activities wherein synthesis of $PI(4,5)P_2$ induces E peptide relocation from the aqueous surface to deeper within the interface and, reciprocally, E peptide relocation attenuates $PI(4,5)P_2$ synthesis.

Regulated electrostatic association/dissociation of $PI(4,5)P_2$ and proteins at the membrane interface appears to be an emerging theme in controlling a variety of cell functions. MARCKS and related proteins (e.g., GAP-43, CAP-23) utilize aromatic/basic peptide segments to electrostatically sequester $PI(4,5)P_2$ with a lipid:protein stoichiometry that may reach 3:1 (*24*). Reversible control of this association by calcium/calmodulin and/or protein kinase C may modulate availability of a substantial fraction of cellular $PI(4,5)P_2$ and appears to be an important factor in regulating organization of the cortical actin cytoskeleton (*12*, *38*). Also the activities of a variety of cell surface transporters/channels are regulated by $PI(4,5)P_2$ (*46*), and in certain cases, mutagenesis studies have implicated protein segments enriched in basic and

nonpolar amino acids in the interaction (*47*−*49*). If our ongoing studies validate the interaction of PI(4,5)P_2 with intact SCAMP2, we will need to address whether the association serves to regulate the availability of PI(4,5)P_2 or to modulate the functions of the SCAMP. Finally, the common electrostatic association of PI(4,5)P_2 with E peptides of SCAMPs 1 and 2 (Figure 2) suggests that we should consider the potential roles of analogous interactions involving other SCAMPs, other PIPs, and other intracellular sites where SCAMPs reside.

ACKNOWLEDGMENT

We are grateful to Payne Chang, Meyer Jackson, and Edwin Chapman (University of Wisconsin) for providing the computer program used for analyzing amperometric recordings and PC12 cells used in amperometry experiments. We thank Derek Persons (St. Jude's Children's Research Hospital) for providing the pIRES-EGFP vector used for PC12 cell transfection. We also thank Anna Castle, University of Virginia, for advice and assistance in cell transfection experiments.

SUPPORTING INFORMATION AVAILABLE

Proton magnetic resonance assignments for SCAMP E peptide in solution and in bicelles along with information regarding solution and bicelle conditions. This material is available free of charge via the Internet at http://pubs.acs.org.

REFERENCES

1. Di Paolo, G., and De Camilli, P. (2006) Phosphoinositides in cell regulation and membrane dynamics, *Nature 443*, 651−657.
2. De Matteis, M. A., and Godi, A. (2004) Protein-lipid interactions in membrane trafficking at the Golgi complex, *Biochim. Biophys. Acta 1666*, 264−274.
3. McLaughlin, S., Wang, J., Gambhir, A., and Murray, D. (2002) PIP(2) and proteins: interactions, organization, and information flow, *Annu. Rev. Biophys. Biomol. Struct. 31*, 151−175.
4. Holz, R. W., Hlubek, M. D., Sorensen, S. D., Fisher, S. K., Balla, T., Ozaki, S., Prestwich, G. D., Stuenkel, E. L., and Bittner, M. A. (2000) A pleckstrin homology domain specific for phosphatidylinositol 4, 5-bisphosphate (PtdIns-4,5-P2) and fused to green fluorescent protein identifies plasma membrane PtdIns-4,5-P2 as being important in exocytosis, *J. Biol. Chem. 275*, 17878−17885.
5. Aikawa, Y., and Martin, T. F. (2003) ARF6 regulates a plasma membrane pool of phosphatidylinositol(4,5)bisphosphate required for regulated exocytosis, *J. Cell Biol. 162*, 647−659.
6. Hay, J. C., and Martin, T. F. (1993) Phosphatidylinositol transfer protein required for ATP-dependent priming of Ca(2+)-activated secretion, *Nature 366*, 572−575.
7. Hay, J. C., Fisette, P. L., Jenkins, G. H., Fukami, K., Takenawa, T., Anderson, R. A., and Martin, T. F. (1995) ATP-dependent inositide phosphorylation required for Ca(2+)-activated secretion, *Nature 374*, 173−177.
8. Milosevic, I., Sorensen, J. B., Lang, T., Krauss, M., Nagy, G., Haucke, V., Jahn, R., and Neher, E. (2005) Plasmalemmal phosphatidylinositol-4,5-bisphosphate level regulates the releasable vesicle pool size in chromaffin cells, *J. Neurosci. 25*, 2557−2565.
9. Grishanin, R. N., Kowalchyk, J. A., Klenchin, V. A., Ann, K., Earles, C. A., Chapman, E. R., Gerona, R. R., and Martin, T. F. (2004) CAPS acts at a prefusion step in dense-core vesicle exocytosis as a PIP2 binding protein, *Neuron 43*, 551−562.
10. Bai, J., Tucker, W. C., and Chapman, E. R. (2004) PIP2 increases the speed of response of synaptotagmin and steers its membrane-penetration activity toward the plasma membrane, *Nat. Struct. Mol. Biol. 11*, 36−44.
11. Gong, L. W., Di Paolo, G., Diaz, E., Cestra, G., Diaz, M. E., Lindau, M., De, Camilli, P., and Toomre, D. (2005) Phosphatidylinositol phosphate kinase type I gamma regulates dynamics of large dense-core vesicle fusion, *Proc. Natl. Acad. Sci. U.S.A. 102*, 5204−5209.
12. Laux, T., Fukami, K., Thelen, M., Golub, T., Frey, D., and Caroni, P. (2000) GAP43, MARCKS, and CAP23 modulate PI(4,5)P(2) at plasmalemmal rafts, and regulate cell cortex actin dynamics through a common mechanism, *J. Cell Biol. 149*, 1455−1472.
13. Aoyagi, K., Sugaya, T., Umeda, M., Yamamoto, S., Terakawa, S., and Takahashi, M. (2005) The activation of exocytotic sites by the formation of phosphatidylinositol 4,5-bisphosphate microdomains at syntaxin clusters, *J. Biol. Chem. 280*, 17346−17352.
14. Brand, S. H., and Castle, J. D. (1993) SCAMP 37, a new marker within the general cell surface recycling system, *EMBO J. 12*, 3753−3761.
15. Castle, A., and Castle, D. (2005) Ubiquitously expressed secretory carrier membrane proteins (SCAMPs) 1-4 mark different pathways and exhibit limited constitutive trafficking to and from the cell surface, *J. Cell Sci. 118*, 3769−3780.
16. Fernandez-Chacon, R., and Sudhof, T. C. (2000) Novel SCAMPs lacking NPF repeats: ubiquitous and synaptic vesicle-specific forms implicate SCAMPs in multiple membrane-trafficking functions, *J. Neurosci. 20*, 7941−7950.
17. Fernandez-Chacon, R., Alvarez de Toledo, G., Hammer, R. E., and Sudhof, T. C. (1999) Analysis of SCAMP1 function in secretory vesicle exocytosis by means of gene targeting in mice, *J. Biol. Chem. 274*, 32551−32554.
18. Guo, Z., Liu, L., Cafiso, D., and Castle, D. (2002) Perturbation of a very late step of regulated exocytosis by a secretory carrier membrane protein (SCAMP2)-derived peptide, *J. Biol. Chem. 277*, 35357−35363.
19. Liu, L., Guo, Z., Tieu, Q., Castle, A., and Castle, D. (2002) Role of secretory carrier membrane protein SCAMP2 in granule exocytosis, *Mol. Biol. Cell 13*, 4266−4278.
20. Liu, L., Liao, H., Castle, A., Zhang, J., Casanova, J., Szabo, G., and Castle, D. (2005) SCAMP2 interacts with Arf6 and phospholipase D1 and links their function to exocytotic fusion pore formation in PC12 cells, *Mol. Biol. Cell 16*, 4463−4472.
21. Caumont, A. S., Vitale, N., Gensse, M., Galas, M. C., Casanova, J. E., and Bader, M. F. (2000) Identification of a plasma membrane-associated guanine nucleotide exchange factor for ARF6 in chromaffin cells. Possible role in the regulated exocytotic pathway, *J. Biol. Chem. 275*, 15637−15644.
22. Vitale, N., Chasserot-Golaz, S., Bailly, Y., Morinaga, N., Frohman, M. A., and Bader, M. F. (2002) Calcium-regulated exocytosis of dense-core vesicles requires the activation of ADP-ribosylation factor (ARF)6 by ARF nucleotide binding site opener at the plasma membrane, *J. Cell Biol. 159*, 79−89.
23. Hubbard, C., Singleton, D., Rauch, M., Jayasinghe, S., Cafiso, D., and Castle, D. (2000) The secretory carrier membrane protein family: structure and membrane topology, *Mol. Biol. Cell 11*, 2933−2947.
24. Wang, J., Gambhir, A., Hangyas-Mihalyne, G., Murray, D., Golebiewska, U., and McLaughlin, S. (2002) Lateral sequestration of phosphatidylinositol 4,5-bisphosphate by the basic effector domain of myristoylated alanine-rich C kinase substrate is due to nonspecific electrostatic interactions, *J. Biol. Chem. 277*, 34401−34412.
25. Ellena, J. F., Moulthrop, J., Wu, J., Rauch, M., Jaysinghne, S., Castle, J. D., and Cafiso, D. S. (2004) Membrane position of a basic aromatic peptide that sequesters phosphatidylinositol 4,5 bisphosphate determined by site-directed spin labeling and high-resolution NMR, *Biophys. J. 87*, 3221−3233.
26. Grassetti, D. R., and Murray, J. F., Jr. (1967) Determination of sulfhydryl groups with 2,2′- or 4,4′-dithiodipyridine, *Arch. Biochem. Biophys. 119*, 41−49.
27. Ellena, J. F., Obraztsov, V. V., Cumbea, V. L., Woods, C. M., and Cafiso, D. S. (2002) Perfluorooctyl bromide has limited membrane solubility and is located at the bilayer center. Locating small molecules in lipid bilayers through paramagnetic enhancements of NMR relaxation, *J. Med. Chem. 45*, 5534−5542.
28. Wang, C. T., Grishanin, R., Earles, C. A., Chang, P. Y., Martin, T. F., Chapman, E. R., and Jackson, M. B. (2001) Synaptotagmin modulation of fusion pore kinetics in regulated exocytosis of dense-core vesicles, *Science 294*, 1111−1115.
29. Chung, S. H., Joberty, G., Gelino, E. A., Macara, I. G., and Holz, R. W. (1999) Comparison of the effects on secretion in chromaffin and PC12 cells of Rab3 family members and mutants. Evidence that inhibitory effects are independent of direct interaction with Rabphilin3, *J. Biol. Chem. 274*, 18113−18120.

30. Wang, C. T., Bai, J., Chang, P. Y., Chapman, E. R., and Jackson, M. B. (2006) Synaptotagmin-Ca2+ triggers two sequential steps in regulated exocytosis in rat PC12 cells: fusion pore opening and fusion pore dilation, *J. Physiol. 570*, 295−307.
31. Colliver, T. L., Hess, E. J., Pothos, E. N., Sulzer, D., and Ewing, A. G. (2000) Quantitative and statistical analysis of the shape of amperometric spikes recorded from two populations of cells, *J. Neurochem. 74*, 1086−1097.
32. Bai, J., Wang, C. T., Richards, D. A., Jackson, M. B., and Chapman, E. R. (2004) Fusion pore dynamics are regulated by synaptotagmin*t-SNARE interactions, *Neuron 41*, 929−942.
33. Wimley, W. C., Creamer, T. P., and White, S. H. (1996) Solvation energies of amino acid side chains and backbone in a family of host-guest pentapeptides, *Biochemistry 35*, 5109−5124.
34. Rauch, M. E., Ferguson, C. G., Prestwich, G. D., and Cafiso, D. S. (2002) Myristoylated alanine-rich C kinase substrate (MARCKS) sequesters spin-labeled phosphatidylinositol 4,5-bisphosphate in lipid bilayers, *J. Biol. Chem. 277*, 14068−14076.
35. Windrem, D. A., and Plachy, W. Z. (1980) The diffusion-solubility of oxygen in lipid bilayers, *Biochim. Biophys. Acta 600*, 655−665.
36. Wang, J., Arbuzova, A., Hangyas-Mihalyne, G., and McLaughlin, S. (2001) The effector domain of myristoylated alanine-rich C kinase substrate binds strongly to phosphatidylinositol 4,5-bisphosphate, *J. Biol. Chem. 276*, 5012−5019.
37. Travis, E. R., and Wightman, R. M. (1998) Spatio-temporal resolution of exocytosis from individual cells, *Annu. Rev. Biophys. Biomol. Struct. 27*, 77−103.
38. McLaughlin, S., and Murray, D. (2005) Plasma membrane phosphoinositide organization by protein electrostatics, *Nature 438*, 605−611.
39. Victor, K., J. Jacob, and D. S. Cafiso. 1999. Interactions controlling the membrane binding of basic protein domains: phenylalanine and the attachmentof the myristoylated alanine-rich C-kinase substrate protein to interfaces. *Biochemistry 38*, 12527−12536.
40. Ben-Tal, N., Honig, B., Peitzsch, R. M., Denisov, G., and McLaughlin, S. (1996) Binding of small basic peptides to membranes containing acidic lipids: theoretical models and experimental results, *Biophys. J. 71*, 561−575.
41. Wang, J., Gambhir, A., McLaughlin, S., and Murray, D. (2004) A computational model for the electrostatic sequestration of PI-(4,5)P2 by membrane absorbed basic peptides. *Biophys. J. 86*, 1969−1986.
42. Singleton, D. R., Wu, T. T., and Castle, J. D. (1997) Three mammalian SCAMPs (secretory carrier membrane proteins) are highly related products of distinct genes having similar subcellular distributions, *J. Cell Sci. 110* (Part 17), 2099−2107.
43. Wu, T. T., and Castle, J. D. (1997) Evidence for colocalization and interaction between 37 and 39 kDa isoforms of secretory carrier membrane proteins (SCAMPs), *J. Cell Sci. 110* (Part 13), 1533−1541.
44. Martin, T. F. (2003) Tuning exocytosis for speed: fast and slow modes, *Biochim. Biophys. Acta 1641*, 157−165.
45. Sorensen, J. B. (2004) Formation, stabilisation and fusion of the readily releasable pool of secretory vesicles, *Pfluegers Arch. 448*, 347−362.
46. Suh, B. C., and Hille, B. (2005) Regulation of ion channels by phosphatidylinositol 4,5-bisphosphate, *Curr. Opin. Neurobiol. 15*, 370−378.
47. Hoshi, T., Zagotta, W. N., and Aldrich, R. W. (1990) Biophysical and molecular mechanisms of Shaker potassium channel inactivation, *Science 250*, 533−538.
48. Oliver, D., Lien, C. C., Soom, M., Baukrowitz, T., Jonas, P., and Fakler, B. (2004) Functional conversion between A-type and delayed rectifier K+ channels by membrane lipids, *Science 304*, 265−270.
49. Prescott, E. D., and Julius, D. (2003) A modular PIP2 binding site as a determinant of capsaicin receptor sensitivity, *Science 300*, 1284−1288.

BI701121J